International Journal of Chemical Research and Development
www.chemicaljournal.in
Online ISSN: 2664-6560; Print ISSN: 2664-6552; Impact Factor: RJIF 5.42
Received: 19-05-2020; Accepted: 05-06-2020; Published: 23-06-2020
Volume 2; Issue 1; 2020; Page No. 24-33

Physico-mechanical properties and microstructure of Portland cement pastes replaced by corn stalk ash (CSA)

HHM Darweesh
Refractories, Ceramics and Building Materials Department, National Research Centre, Cairo, Egypt

DOI: https://doi.org/10.33545/26646552.2020.v2.i1a.18

Abstract
Corn stralk ash (CSA) is considered as one of the most recent abundant, renewable and green supplementary cementitious materials, which in turn is an effective approach to reduce the quantity of cement portion in blended cement. This in turn minimized the environmental pollution and also the CO_2↑ emission. In the present study, the influence of CSA on the physical, chemical and mechanical properties as well as the microstructure of hydrated cement pastes containing various ratios of CSA up to 90 days was evaluated. Several techniques were carried out to confirm the obtained results of the newly formed hydration products as heat of hydration, and SEM images. It is concluded that the cement could be partially replaced by CSA without any adverse response on the properties of cement pastes. The SEM images showed that the content of the calcium dioxide or free lime is obviously decreased with CSA or may be disappeared.

Keywords: cement, corn stalk ash, pozzolanic activity, setting, free lime, density, porosity, strength, SEM

1. Introduction

1.1. Scope of the problem

In many agricultural countries like Egypt, Sudan, Tunisia, Morocco, China, India and many others, emissions of gaseous and particulate pollutants from open burning of agricultural wastes are one of the most important sources of air pollution. In Egypt, the production of corn is concentrated in a limited agricultural area around the Nile valley, where nearly about 10 million tons of corn stalk is produced annually. Always, this is often creating a large volume of corn byproducts like hills. Often, an uncontrolled burning of corn stalk residues was done for its disposal. Random burning of either corn stalk or even any kinds of agro/wastes that creates what is known as "Black Cloud" which is very dangerous to the environment. The seasonal and highly localized massive burning usually generated an excessive air pollution that lowers air quality in the surrounding megacity of Cairo. This has become a serious health concern for citizens and authorities [1-5]. The biomass power plant, among other alternatives, is widely used for the disposal of biomass wastes like barely, wheat straw [6], corn stalk [3, 6], sun flower stalk [6, 7] and rice husks [5, 8-14] so as to solve the environmental problems. Accordingly, the corn straw (CS) is often containing much more active silica and alumina which helps and possesses a good pozzolanic reactivity with the evolved Ca $(OH)_2$ from the hydration of calcium silicate phases of the cement (C_3S and β-C_2S) with water. So, it can be potentially reused as a supplementary cementitious material to partially replace cement [9-18].Previous works [19-23] had reported that the addition of traditional supplementary cementitious materials could improve the physical, chemical and mechanical properties. Since 3-4 decades, the pozzolanic cements are widely used worldwide. Such cements are successfully employed for their economical, ecological and technological interest, i.e. Reduction of energy consumption and CO_2↑emission [11-15, 20-24].

1.2. Objectives of the work

The main objectives of this work are the evaluation and follow the characteristics of Ordinary Portland cement containing corn stalk ash hydrated up to 90 days. The heat of hydration, setting time, free lime, density, porosity and strength development were investigated at all hydration stages. The obtained results were confirmed with scanning electron microscopy (SEM) technique.

2. Experimental and Methods

2.1. Raw materials

The used raw materials in the present research are Ordinary Portland cement (OPC Type I- CEM I 42,5R) with blaine surface area 3400 cm^2/g, and corn stalk (CS) as a source of nanosilica with fineness 6155 cm^2/g. The blaine surface area was conducted by the "Air Permeability Apparatus". The OPC sample was supplied from Sakkara cement factory, Giza, Egypt, and its commercial name is known as "Asmant El-Momtaz", while CS sample was supplied by a local plant, Bani Suef, Egypt. The CS was first processed and washed with running water, and also with distilled water, and then let to dry under sun and open air for few days. The dried CS was subjected for firing at 700 ºC inside a suitable muffle furnace for one hour soaking time to produce what is known as corn stalk ash (CSA). Then, the resulting CSA was screened to pass through 300 µm standard sieve.
The mineralogical phase composition of the used OPC as calculated from Bogue equations [2, 4-6, 15, 16, 19, 24] is given in Table 1.The chemical composition of the OPC and CSA as measured by X-ray florescence technique (XRF) is shown in Table 2, while the mix composition is illustrated in Table 3. The CSA particles are amorphous and crystalline. It is mainly composed of a large

Percentage of nano-SiO_2 and a lower percentage of nano-Al_2O_3.

Table 1: Mineralogical composition of the used OPC sample, mass %.

Phase Material	C_3S	β-C_2S	C_3A	C_4AF
OPC	43.01	30.00	5.65	9.58

Table 2: Composisition of the used raw materials, mass %.

Oxide Material	SiO_2	Al_2O_3	Fe_2O_3	CaO	MgO	MnO	SO_3	Na_2O	P_2O_5	K_2O	LOI
OPC	20.12	4.25	1.29	63.13	1.53	0.36	2.54	0.55	0.19	0.30	2.64
CSA	66.47	8.29	3.13	5.46	4.16	0.02	0.51	2.52	----	2.06	1.02

Table 3: The batch composition of cement mixtures, mass %.

Batch Material	C0	C1	C2	C3	C4	C5	C6	C7	DensitY, g/cm^3	Bl. Finene, cm^2/g	Specific gravity
OPC	100	97	94	91	88	85	82	79	2.2215	3400	3.14
CSA	----	3	6	9	12	15	18	21	2.6546	6810	3.31
Fineness, cm^2/g	3400	3510	3732	3843	4035	4136	4308	4455			

2.2. Preparation and methods

There are seven cement mixtures from OPC and CSA as 100:0, 96:4, 92:8, 88:12, 84:16, 80:20 and 76:24 having the symbols: C0, C1, C2, C3, C4, C5 and 65, respectively. The blending process of the various cement batches was firstly done in a porcelain ball mill using three balls for two hours to assure the complete homogeneity of all cement batches. To improve the dispersion of the different cement batches, a certain percentage of Na-lignosulphonate admixture must be added to all cement mixtures with the mixing water during casting of cement pastes to avoid the agglomeration of the nanoparticles of cement powder and CSA. Sodium lignosulfonate admixture was applied due to its higher activity than other conventional ones (Fig. 1).

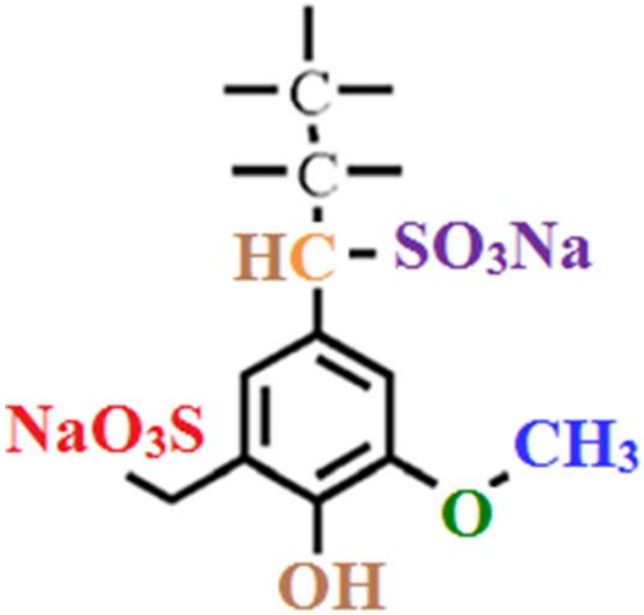

Fig 1: The chemical structure of sodium lignosulphonate.

The standard water of consistency [25] and setting times [26, 27] of the various cement pastes were directly measured using Vicat Apparatus (Fig. 2), and then the water of consistency could be calculated from the following relation:

$$WC, \% = A / C \times 100 \quad (1)$$

Where, A is the amount of water taken to produce a suitable paste, C is the amount of cement mix (300 g).

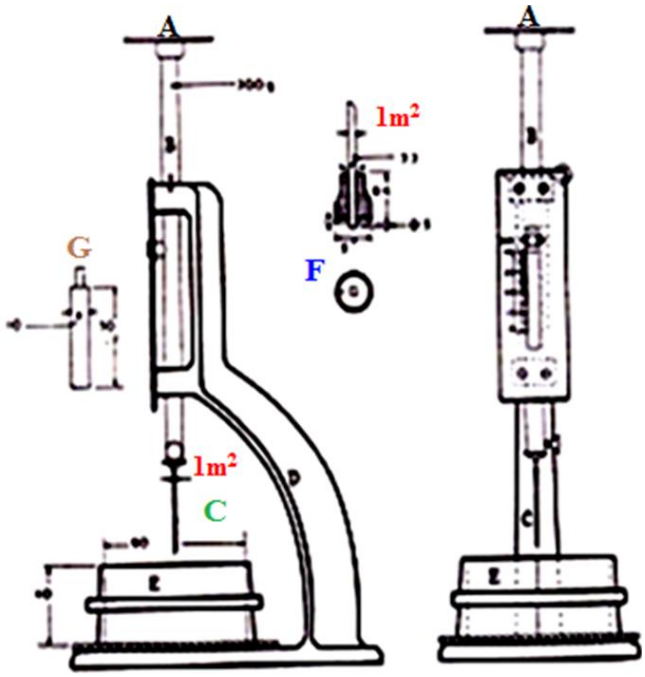

Fig 2: Vicat Apparatus for determining water of consistency and setting times.

During mixing, the correct predetermined w/c-ratio (water of consistency) was poured into the cement portion inside the mixer step by step, and then the mixer was run for 5 minutes at an average speed of 10 rpm in order to have perfect homogenous pastes. Before casting of cement cubes, the moulds were delt with a thin film of a motor engine oil to facilitate the release of the cement cubes from the moulds during the de-moulding process. The cement pastes were then moulded into one inch cubic stainless steel moulds (2.5 x 2.5 x 2.5 cm^3) using about 500 g from the cement powder batch, vibrated manually for three minutes, and then on a mechanical vibrator for another three minutes to remove all air bubbles tapped inside the cement pastes. The moulds were filled to the top surface and smoothed with a flat stainless steel trowel or spatula to obtain a flat and smooth surface [7, 8, 11, 14]. After casting of samples, they were covered with a wet sheet during the first 24 hours to prevent moisture loss. The moulds were then kept in a humidity chamber for 24 hours under 95 ± 1 relative humidity (RH), and room temperature (23 ± 1), demoulded in the following day and soon cured by the total immersion in water at an ambient laboratory temperature till the time of testing for heat of hydration, bulk density, apparent porosity, compressive strength, combined water and free lime

Contents at 1, 3, 7, 28 and 90 days. This is necessary for the cement cubes as it facilitates the proper hydration of cement phases.

The bulk density (BD) and apparent porosity (AP) of the hardened cement pastes [4, 5, 7, 15, 16-19, 24] were calculated from the following equations:

$$B.D, (g/cm3) = W1/ (W1–W2) \times 1 \quad (2)$$

$$A.P, \% = (W1 – W3) / (W1–W2) \times 100 \quad (3)$$

Where, W1, W2 and W3 are the saturated, suspended and dry weights, respectively. The compressive strength (CS) of the various hardened cement pastes [28, 29] was measured and calculated from the following relation:

$$CS=L (KN)/Sa (cm2) KN/m2 \times 102 (Kg/cm2)/10.2 (MPa) \quad (4)$$

Where, L is the load taken, Sa is the surface area. Thereafter, about 10 grams of the broken specimens were first well ground, dried at 105ºC for 30 min. and then were placed in a solution mixture of 1:1 methanol: acetone to stop the hydration [30-33]. The kinetics of hydration in terms of chemically bound water and free lime contents were also measured. About one gram of the sample was first dried at 105ºC for 24 hours and then the bound water content [30, 32, 33] at each hydration age was determined on the basis of ignition loss at 1000ºC for 30 minutes soaking where about 10 grams of the broken specimens from the determination of compressive strength were first well ground, dried at 105ºC for 30 minutes and then were placed in a solution mixture of 1:1 methanol: acetone to stop the hydration [2, 24, 34]. The kinetics of hydration in terms of chemically combined water and free lime contents were also measured. About one gram of the sample was first dried at 105ºC for 24 hours, and then the chemically-combined water content (CWn) at each hydration age was determined on the basis of ignition loss at 1000ºC for 30 minutes [24, 35] from the following equation:

$$CWn, \% = W1\text{-}W2/W2 \times 100 \quad (5)$$

Where, CWn, W1 and W2 are combined water content, weight of sample before and after ignition, respectively. The free lime content (FLn) of the hydrated samples pre-dried at 105°C for 24 hours was also determined. About 0.5 g sample + 40 ml ethylene glycol → heating to about 20 minutes without boiling. About 1–2 drops of pH indicator were added to the filtrate and then titrated against freshly prepared 0.1N HCl until the pink colour disappeared. The 0.1 N HCl was prepared using the following equation:

$$V1 = N \times V2 \times W \times 100/D \times P \times 1000 \quad (6)$$

Where, V1 is the volume of HCl concentration, V2 is the volume required, N is the normality required, W is the equivalent weight, D is the density of HCl concentration and P is the purity (%). The heating and titration were repeated several times until the pink colour did not appear on heating. The free lime content [24, 35] was calculated from the following relation:

$$FLn, \% = (V \times 0.0033/1) \times 100 \quad (7)$$

Where, FLn and V are the free lime content and the volume of 0.1 N HCl taken on titration, respectively. The obtained results were then confirmed by scanning electron microscopy (SEM). The XRF analysis was carried out in the National Research Centre. The SEM microscopy was done for some selected samples by using JEOL–JXA–840 electron analyzer at accelerating voltage of 30 KV. The fractured surfaces were fixed on Cu-kα stubs by carbon paste and then coated with a thin layer of gold.

3. Results and Discussion

3.1. Chemical composition of cement and corn stalk ash

The chemical composition of CSA in comparison with some pozzolanic materials is shown in Table 4. According to ASTM C618, 2015a [36], the sum of SiO_2 + Al_2O_3 + Fe_2O_3 requirement for a standard pozzolana is 70% which is more with that of CSA sample (77.89 %). The standard specification also sets maximum limits of SO_3 and Loss on Ignition (LOI) as 4 % and 10%, respectively. As shown in Table 4, the SO_3 content of CSA sample was found below the acceptable limit, where SO_3 is 0.51 % while LOI was negligible (1.02).

Therefore, the CSA powder is expected to be as a pozzolanic material in the cementitious system.

Table 4: Chemical composition of CSA in comparison with GbfS, SF, Pfa, SCBA, SDA, SFSA and WSA.

Materials Oxides	CSA	GbfS	SF	Pfa	SCBA	SDA	SFSA	WSA
SiO_2	66.47	36	90.9	59.2	70.83	66.17	63.83	69.36
Al_2O_3	8.29	12	1.1	25.6	9.21	4.35	6.68	5.97
Fe_2O_3	3.13	1	1.5	2.9	1.95	2.36	2.79	2.15
CaO	5.46	38	0.7	1.1	8.16	10.06	5.46	7.28
MgO	4.16	----	0.8	0.3	1.32	4.41	6.23	1.44
MnO	0.02	1.31	----	1.05	----	2.19	----	----
Na_2O	2.52	0.3	----	0.2	0.12	0.08	0.24	0.31
K_2O	2..06	-----	-----	0.9	1.65	0.12	1.17	1.11
SO_3	0.51	8.11	0.4	0.3	1.47	0.30	1.11	1.27
P_2O_5	----	2.16	----	0.14	----	0.46	----	----
LOI	1.02	1.0	3.0	1.4	6.91	0.84	3.35	2.37

3.2. Physical properties

The physical properties of the used OPC and CSA samples are listed in Table 5 and the relationship between the blaine fineness, density and specific gravity of the used OPC and CSA samples is represented in Fig. 3.

The surface area or Blaine fineness of CSA is sharply higher, while it's the density is slightly higher than those of the OPC, whereas its specific gravity is slightly lower.

The data shown in Tables 4 and 5 confirmed that the CSA could be used as a mineral admixture for cement pastes, mortars or even concretes [4, 33, 37, 38].

The relationship between the surface area or fineness of the OPC (C0) and the various cement batches incorporated CSA (C1-C7) is graphically represented in Fig. 4. It is clear that as the CSA content increased in the cement batch, the surface area or fineness of the whole mix increased too as shown in Table 3 and Fig. 4. This is mainly due to the presence of many nanoparticles of CSA.

Table 5: Physical properties of the used OPC and CSA samples.

Property Raw materials	Density, g/cm^3	Blaine Finenes, cm^2/g	Specific gravity
OPC	2.2215	3400	3.14
CSA	2.6546	6810	2.81

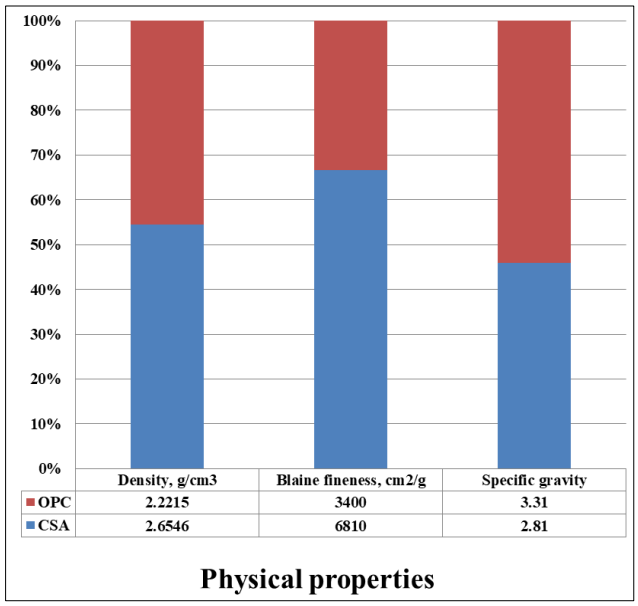

Fig 3: Relationship between Density, Blaine surface area and specific gravity of OPC and CSA samples.

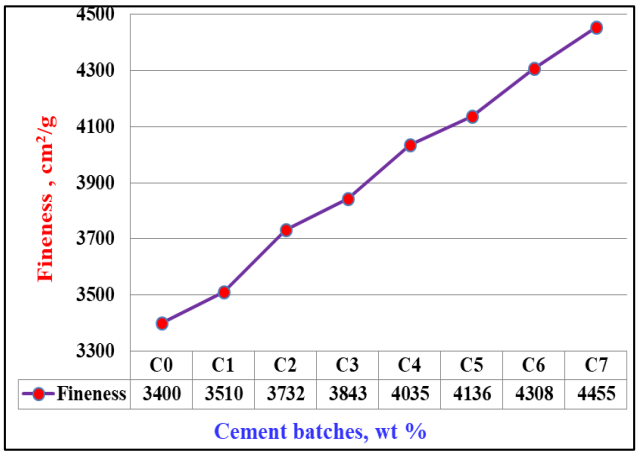

Fig 4: Relationship between the fineness of the different cement batches containing CSA

3.3. Water of consistency and setting times

Figure 5 illustrates the water of consistency and setting times (initial and final) of the OPC (C0) and the various cement pastes containing CSA (C1-C7). It is obvious that the water of consistency increased gradually as the CSA content increased to form suitable cement pastes. This is essentially attributed to the increase in the rate of hydration process in the presence of excess water [24, 30, 31].

On the other hand, in spite of the gradual increase of water of consistency, the setting times decreased step by step with CSA content. This is mainly due to the surrounded climatic factors, particularly the high atmospheric Lab. Temperature (37 °C) during testing [2, 3, 6, 7, 16, 18].

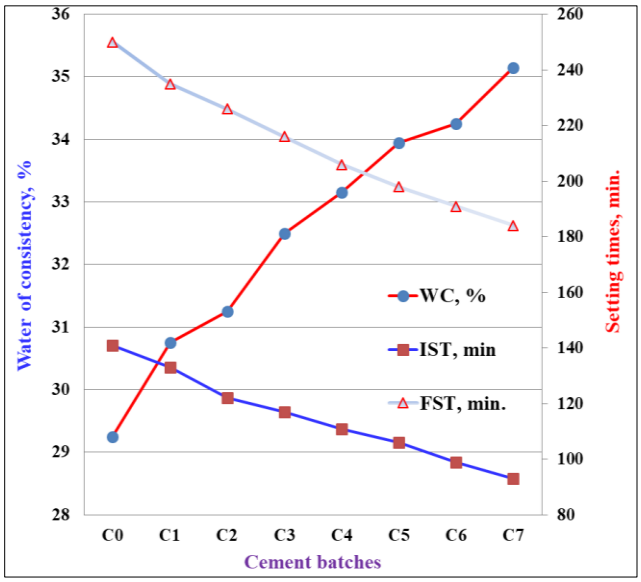

Fig 5: Water of consistency and setting times of the various cement pastes (C0-C7).

3.4. Heat of hydration

The heat of hydration of the various cement pastes containing CSA (C0-C7) is graphically plotted as a function of hydration times for 1, 3, 7, 28 and 90 days in Fig. 6. Results illustrated that as soon as the various cement powders become in contact with water, the heat of hydration of all cement pastes was soon released. The rate of released heat increased as the hydration time proceeded up to 90 days. The same trend was displayed for all cement pastes. This was followed by the release of heat [2, 24, 35]. This is mainly contributed to the increase of the rate of hydration of cement pastes as well as the pozzolanic reactions between the constituents of the cement and those of the CSA. Furthermore, the rate of the released heat of hydration sharply enhanced at early ages up to 7 days. This is essentially attributed to the activation effect of the hydration reaction mechanism of C_3S by the very fine and active CSA particles [39-41]. At older ages (28-90 days), the rate of hydration reaction and also the evolved heat also slightly increased. This may be due to the activation action mechanism of β-C_2S by the fine CSA particles [2, 3, 5-7, 19, 21, 27]. The heat of hydration increased as the CSA content increased only up to 18 wt % CSA (C1-C6). But with any further increase of CSA (C7), a sudden sharp decrease of heat of hydration lower than those of the blank (G0) was recorded. This was contributed to the dilution effect of the main binding material (OPC), and the retardation effect of the higher quantity of CSA at the expense of the OPC.

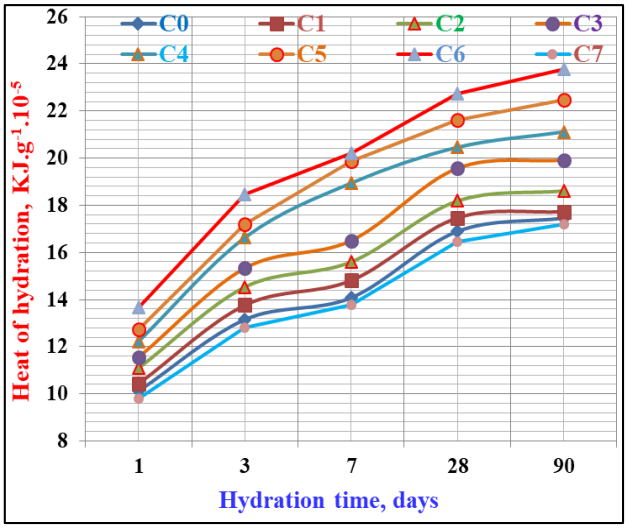

Fig 6: Heat of hydration of the various cement pastes (C0-C7) hydrated up to 90 days.

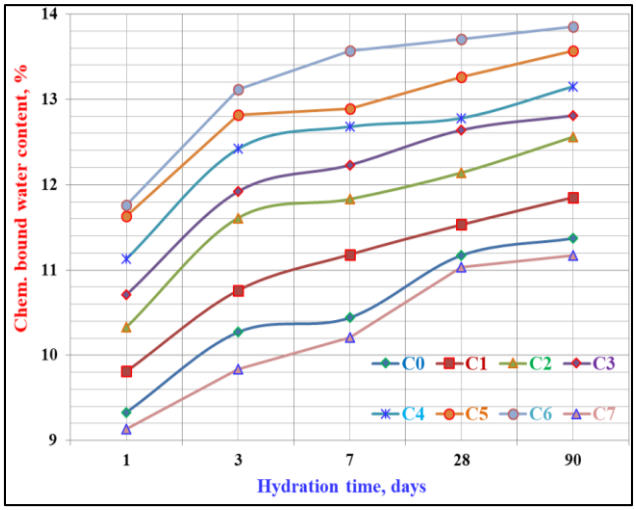

Fig 7: Chemically-bound water contents of the various cement pastes (C0-C7) hydrated up to 90 days.

3.5. Chemically-bound water contents

The chemically-bound water contents of the different cement pastes containing CSA (C0-C7) are plotted versus hydrations time up to 90 days in Fig. 7. For all cement pastes, the bound water content proceeded as the hydration time progressed up to 90 days. This is essentially attributed to the hydration of the main cement phases, especially C_3S, C_3A and C_4AF at early ages of hydration up to 7 days, whereas β-C_2S often hydrates at later ages from 28 days onward [2,5,7,8,12,17,27]. The bound water contents slightly increased as the CSA content increased only up to 18 wt %, and then suddenly decreased sharply with further increase of CSA nearly at all hydration ages, i.e. the cement blends C1, C2, C3, C5 and C6 containing 3, 6, 9, 12, 15 and 18 wt % CSA, respectively are slightly higher than those of the pure OPC (C0). This is primarily due to the activation effect of the nano- and active silica of the CSA [6, 12, 15, 20, 21]. Moreover, the pozzolanic reactivity of CSA through which its constituents can react with the Ca $(OH)_2$ coming from the hydration of C_3S at early stages of hydration and β-C_2S at later stages to produce addition CSH. The bound water contents of C7 were becoming lower than those of the control mix (C0). This may be due to that the higher amounts of CSA hindered and be as an obstacle for the hydration of the phases of the blank (C0). Also, the deficiency of the main hydrating material is the main reason for the decrease of bound water [3, 7, 15, 17, 20, 21, 27]. Accordingly, it can be concluded that the optimum addition of CSA does not exceed 18 wt % because the higher amounts of CSA is undesirable due to its adverse effect, i.e. the higher quantity of CSA must be avoided because it may be hindered the hydration of cement phases.

3.6. Free lime content

Figure 8 indicates the free lime contents of the various cement mixes (C0-C7) hydrated up to 90 days as a function of cement batches. Generally, the free lime contents of the control cement pastes (C0) were gradually increased with the hydration ages up to 90 days indicating an enhancement in the rate of hydration [17, 27]. This is mainly due to the hydration process of calcium silicate phases (C_3S and C_2S) of the cement as follows:

$$3\ C_3S + 6\ H_2O \rightarrow C_3S_2H_3 + 3\ Ca\ (OH)_2 \quad (8)$$

$$2\ \beta\text{-}C_2S + 4\ H_2O \rightarrow C_3S_2H_3 + Ca(OH)_2 \quad (9)$$

As the CSA content enhanced in the cement mixes (C1-C7), the free lime content decreased only up to 18 wt % (C6). But, with further increase of CSA in the cement batch (C7), the free lime contents started to increase gradually as the hydration ages progressed till reach to 90 days. So, the representing curve of free lime contents of C7 was becoming up to that of the blank (C0) at all hydration periods. The increase is due to the normal hydration process of the cement phases, while the decrease is due to the activation power of CSA and its pozzolanic reactions between its active nanosilica and the resulting $Ca(OH)_2$ from the hydration of C_3S at early ages and β–C_2S at later ages of hydration in contact of water. In the cement mixes (C1-C6), the rate of hydration improved and enhanced than in the blank (C0) at all hydration stages. This is certainly attributed to activation effect occurred by CSA and also its pozzolanic reactivity with the free lime released by the cement [2, 3, 7, 12, 17, 21, 23, 27]. The increase of free lime contents recorded by C7 cement pastes decreased the rate of

Hydration. This is due to the lack of the essential hydrating Material because the higher amount of CSA hinders the rate of hydration [3, 17, 23, 27, 29]. The obtained results proved that the CSA acts as a pozzolanic material at all ages of hydration. So, the higher amounts of CSA must be avoided due to its negative response on the physical and chemical properties of the cement [2, 12, 27, 39].

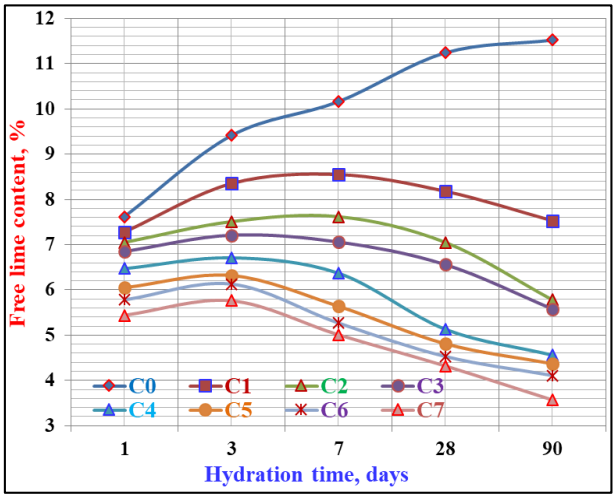

Fig 8: Free lime contents of the various cement pastes (C0-C7) hydrated up to 90 days.

3.7. Bulk density and apparent porosity

Figures 9 and 10 demonstrate the graphs of the bulk density and apparent porosity of the various cement pastes (C0-C7) versus the hydration time up to 90 days. Generally, the bulk density of the various cement mixtures improved and enhanced as the hydration time proceeded up to 90 days, while the apparent porosity decreased. This is mainly due to that as the dry cement batches become in contact with water the hydration process starts to produce CSH and/or CAH, which immediately deposited in the pore system of samples leading to a decrease in the porosity and an increase of bulk density [3, 17, 27, 39], i.e. as the hydration time proceeds, the formed hydration products (CSHs) increased too. Therefore, this was reflected positively on both bulk density and apparent porosity [2, 5, 7, 17, 27, 40]. The bulk density of the cement mixes (C1-C6) increased little by little only up to 18 wt % (C6), whereas the apparent porosity decreased, i.e. the bulk density of cement blends C1-C6 are slightly higher than those of the of the blank (C0). This is evidently due to the formation of additional CSH and/or CAH due to the pozzolanic reactions of CSA with the constituents of cement through which the constituents of CSA can react with the free lime, Ca $(OH)_2$ resulting from the hydration of C_3S at early stages of hydration and β-C_2S at later stages to produce additional CSH and/or CAH besides the normal hydration process of cement phases [7, 12, 15, 17, 39, 41]. With further increase of CSA > 18 wt % (C7), the BD started to decreased, while the apparent porosity increased at all hydration times. Due to that, the higher quantity of CSA may obstruct and hinder the hydration process, i.e. it affects adversely and decrease the rate of hydration, but it slightly benefits as a filler. So, the addition of a large amount of CSA at the expense of the main binding material (C0) is undesirable because it was not sufficient for inducing the reaction of cement with nano-active silica of CSA.

Hence, it could be concluded that the CSA is so beneficial to cement that it helps in the hydration process as a pozzolanic material and also as a filling agent [3, 6, 7, 12, 19, 21, 23, 42].

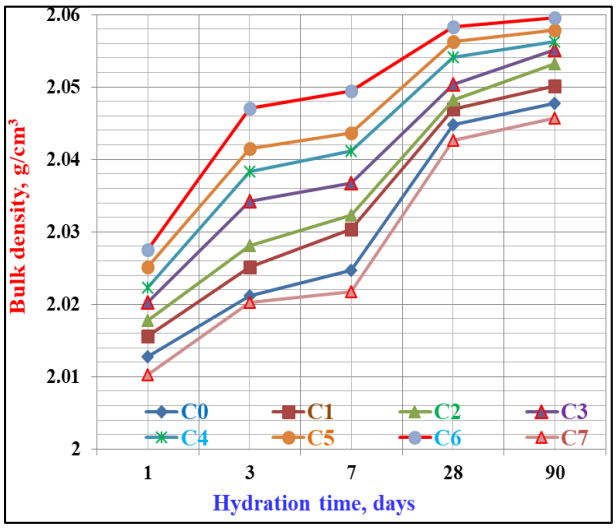

Fig 9: Bulk density of the various cement pastes (C0-C7) hydrated up to 90 days.

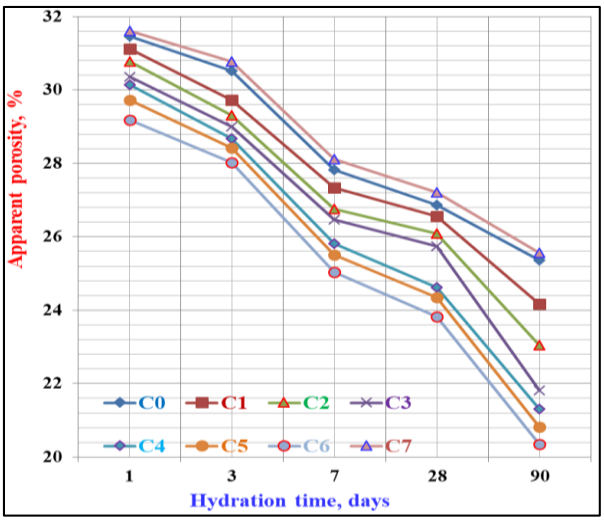

Fig 10: Apparent porosity of the various cement pastes (C0-C7) hydrated up to 90 days.

3.8. Compressive strength

It is well known that the water/cement ratio of cement pastes and concrete affects the workability to a great extent, which in turn affects the strength development of the hardened cement pastes, mortars or concrete, i.e. the decrease of w/c-ratio results in an increase of workability accompanied by an increase in the strength of the hardened cement pastes, and the opposite is correct [12, 17, 27, 39, 40, 42]. Figure 11 shows the graphs of the compressive strength (CS) of the various cement pastes (C0-C7) versus the hydrating time up to 90 days. The compressive strength was generally improved and enhanced gradually as the hydration stage proceeded up to 90 days. This is mainly attributed to the formation of CSH and/or CAH that generally deposited into the pore structure of the hardened cement samples. This results in a decrease in the pore system and an increase in the bulk density.

This in turn improved and enhanced the compaction of the prepared samples, in addition to the good dispersion by the used admixture and the good compaction during moulding. This often reflected positively on the compressive strength. As a result, the compressive strength increased [14, 17, 29, 30, 40]. The compressive strength also enhanced as the CSA content increased in the cement mixture only up to 18 wt % CSA (C6) at all hydration times. This is essentially due to the activation effect and formation of more hydration products that are resulting from the pozzolanic reactions of active nanosilica and nanoalumina of CSA with the free lime evolved from the hydration of C_3S and β–C_2S of cement to produce cubic crystals of hydrogarnet ($C_3A.\ S_2.\ H_n$) as follows:-

$$Al_2O_3 + SiO_2 + Ca\ (OH]_2 \rightarrow C_3A.\ S_2.\ H_n \qquad (10)$$

On the other hand, the decrease of free lime content improves physical, chemical and mechanical properties of the hardened cement pastes (Fig. 6). Therefore, the compressive strength improved and enhanced [30, 35, 36-42]. Hence, this would be led to the segmentation of large capillary pores and nucleation sites due to the continuous deposition of hydration products, i.e. CSH from the normal hydration of cement phases and additional CSH from the pozzolanic reactions of CSA with the released free lime [5-7, 12, 15, 30, 39, 40, 42]. With further increase of CSA > 18 wt %, the compressive strength were suddenly decreased. The is due to the fact that the substitution of larger amount CSA at the expense of the essential cementitious material of the cement could be stood as an obstacle against the normal hydration of cement phases. Consequently, the rate of hydration shortened or declined. Accordingly, this should be reflected negatively on the compressive strength [17, 27, 38-40, 42]. The cement mix (C6) achieved the highest values of compressive strength, whereas that of C7 exhibited the lowest.

On this basis, the cement batch containing 18 % CSA (C6) is considered as the optimum cement batch. Hence, the CSA does not only improve the various characteristics of the OPC, but from an economical point of view, it also reduces the cost of the very expensive OPC production.

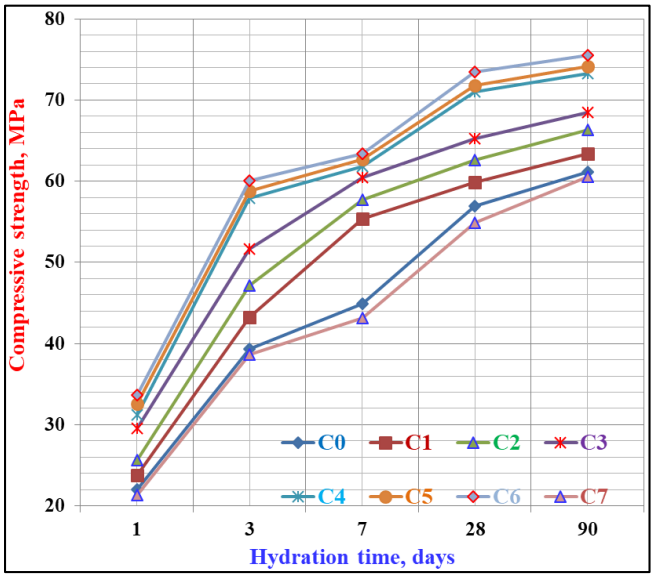

Fig 11: Compressive strength of the various cement pastes (C0-C7) hydrated up to 90 days.

3. 9. Scanning electron microscopy

The SEM microscopy of C0, G3 and C6 hydrated up to 28 days is illustrated in Fig. 12. The ettringite phase is clearly detected in C0 as needles-like crystals (A). Large crystal sheets of CSH and/or CAH are detected with C3, while masses or big crystal s of CSH and/or CAH are formed with C6. In addition, spots and pits of portlandite or free lime are well detected in C0 and C3 samples with variable rates, but they are completely disappeared in C6 sample. This proved that the addition of CSA decreased the free lime content.

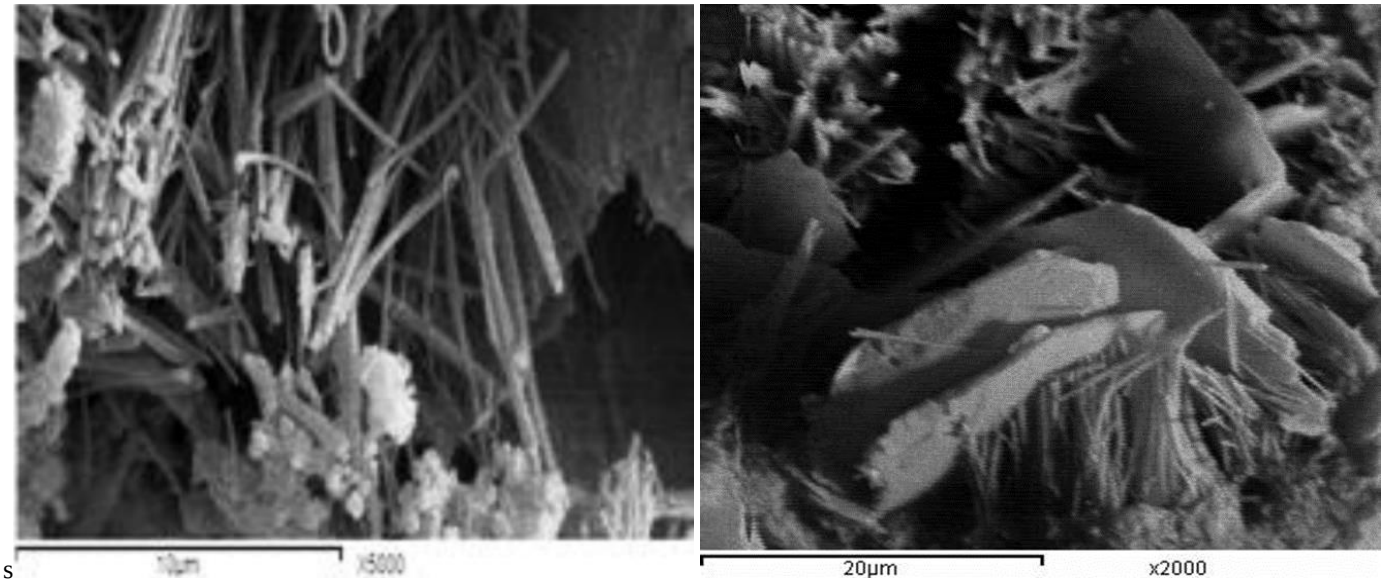

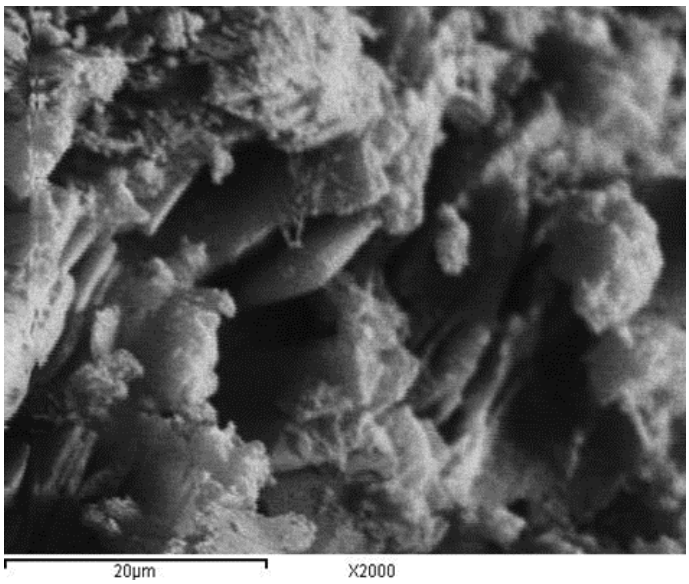

Fig 12: SEM spectroscopy of Cement pastes C0, C3 and C6 hydrated up to 28 days

4. Conclusions

Concerning the findings of the laboratory test results, the following overall conclusions could be obtained

1. The incorporation of the Na-lignosulphonate admixture is the mean cause responsible for the modification and improving most of the physical, chemical and mechanical properties of the hardened cement pastes. The addition of this admixture improves the dispersability and workability of the whole cement mixtures.
2. As the content of active nano-silica particles (CSA) increased in the cement mixture, the Blaine fineness of the whole cement batches increased too.
3. The water of consistency of the blank (C0) was 29.25 %, and its initial and final setting times were 141 and 250 minutes. These values tended to diminish or decrease with the increase of CSA content due to the presence of Na-lignosulphonate admixture, which it is a superplasticizer that reduces largely the mixing water. Furthermore, the high atmospheric temperature during the test.
4. Generally, the heat of hydration, chemically combined water content, bulk density and compressive strength improved and enhanced gradually with the hydration ages up to 90 days. With the increase of CSA content, these properties enhanced only up to 18 wt % (C6), and then decreased suddenly with its further increase.
5. The free lime content of the blank (C0) increased as the hydrating time progressed up to 90 days, while the free lime content of C1 and C2 only increased as the hydration time proceeded up to 7 days, and then decreased. But with C3, C4, C5, C6, and C7, the free lime contents increased only up to 3 days, and then decreased.
6. as the cement powder becomes in contact with water, the apparent porosity was soon diminished and reduced with the replacing up to 18 % CSA (C6) due to activating and filler effects of the nano silica of the CSA, and then raised and enhanced onward with further increase of > 18 wt % CSA due to the reduction of the hydration and pozzolanic reactions.
7. The addition of 18 % CSA (C6) to Portland cement could be Successfully applied without any adverse effects on the physical, chemical and mechanical properties of Portland cement. Therefore, it was selected to be the optimum batch.
8. The SEM images showed the formation of needle like-crystals or ettringite with the blank (C0). Many sheets or mass crystals are detected due the presence of CSA.

5. Acknowledgement

The author wishes to express his deep thanks to National Research Centre for helping to obtain materials, processing, preparing, molding and measuring all of the obtained data of the study, and moreover for financial assistance.

Compliance with ethical standards

The author declines that there is no conflict of interest anywhere.

6. References

1. Eisentraut, ABA. Technology Roadmap Bioenergy for Heat and Power. International Energy Agency, 2012.
2. Darweesh HHM; Abo El-Suoud MR (2019), Palm Ash as a Pozzolanic Material for Portland cement Pastes, To Chemistry Journal. 2019; 4:72-85. http://purkh. com/index. php/tochem
3. Raheem AA, Aedokun SI, Adeyinka EA, Adewole BV. Application of cornstalk ash as partial replacement for cement in the production of interlocking paving stones, International Journal of Engineering Research in Africa. 2017; 30:85-93. https://doi.org/10. 4028/www.scientific. net/JERA.30.85
4. HHM Darweesh. Effect of combination of Some Pozzolanic Wastes on the Properties of Portland cement Pastes, iiC l'italiana del Cemento. 2005; 808(4):298-310.
5. HHM Darweesh, Abo El-Suoud MR. Setting, Hardening and Mechanical Properties of Some Cement / Agrowaste Composites - Part I, American Journal of Mining and Metallurgy. 2014; 2(2):32-40.
6. Binici H, Ortlek E. Engineering properties of concrete made with cholemanite, barite, corn stalk, wheat straw and sunflower stalk ash. European Journal of Engineering and Technology, 2015, 3.

7. Darweesh HHM. Influence of Sun Flower Stalk Ash (SFSA) on the behavior of Portland cement pastes, Results in Engineering, In Press, 2020.
8. Karim MR, Zain MFM, Jamil M. Strength of Mortar and Concrete as Influenced by Rice Husk Ash: A Review, World Applied Sciences Journal. 2012; 19(10):1501-1513.
9. Sadiqul Islam GM, Rahman MH, Kazi N. Waste glass powder as partial replacement of cement for sustainable concrete practice, International Journal of Sustainable Built Environment. 2017; 6:37–44
10. Abu Bakar BH, Ramadhansyah PJ, Megat MA, Johari MA. Effect of rice husk ash fineness on the chemical and physical properties of concrete", Mag. Concr. Res. 2011; 63:313-320.
11. Memon SA, Shaikh MA, Akbar H. Utilization of rice husk ash as a mineral admixture", Constr. Build. Mat. 2011; 25(13):1044-1048.
12. Ettu LO, Ajoku CA, Nwachukwu KC, Awodiji CTG, Eziefula UG. Strength variation of OPC-rice husk ash composites with percentage rice husk ash, Int. J. App. Sci. and Eng. Res. 2013; 2(4):420-424.
13. Kartini K. Rice husk ash-pozzolanic material for sustainability, Int. J. Appl. Sci. Technol. 2011; 1(6):169-178.
14. Antiohos SK, Tapali JG, Zervaki M, Sousa-Coutinho J, Tsimas S, Papadakis VG, *et al*. Low embodied energy cement containing untreated RHA: A strength development and durability study, Const. Build. Materials. 2013; 49:455-463.
15. Darweesh HHM, Abo El-Suoud MR. Influence of sugarcane bagasse ash substitution on Portland cement characteristics, Indian Journal of Engineering. 2019; 16:252-266.
16. Darweesh HHM, Abo El-Suoud MR. Saw dust ash substitution for cement pastes-Part I", American j. of Construction and Building Materials. 2018; 2(1):1-9. http://www.sciencepublishinggroup.com/j/ajcbm DOI: 10.11648/j.ajcbm.20170201.11
17. Hewlett PC, Liska M. Lea's Chemistry of Cement and Concrete, 5th ed., Edward Arnold Ltd., London, England Google Scholar, 2017.
18. S Rukzon, P Chindaprasirt. Utilization of bagasse ash in high-strength concrete, Materials & Design. 2012; 34:45–50. www.elsevier.com/locate/matdes
19. HHM Darweesh, MR Aboel-Suoud. Effect of Agricultural Waste Material on the Properties of Portland Cement Pastes, Journal of Research & Development in Material science. 2020; 13(1):1360-1367.
20. TS Abdulkadir; DO Oyejobi, AA Lawal. Evaluation of Sugarcane Bagasse Ash as a Replacement for Cement in Concrete, Works Acta Tehnica Corviniensis – Bulletin of Engineering (Ilorin: University of Ilorin), 2014, 71–76.
21. Raheem AA, Olasunkanmi BS, Folorunso. Saw Dust Ash as Partial Replacement for Cement in Concrete, Technology and management in construction. 2012; 4(2):474-480. https://doi.org/10.5592/otmcj.2012.2.3
22. Zhang H, Hu J, Qi Y, Li C, Chen J, Wang X, et al. Emission characterization, environmental impact, and control measure of PM2.5 emitted from agricultural crop residue burning in China. Journal of Cleaner Production. 2017; 149:629-635. https://doi.org/10.1016/j.jclepro.2017.02.092
23. Viet-Thien-An Van, Christiane Rößler, Danh-Dai Bui, Horst-Michael Ludwig. Mesoporous structure and pozzolanic reactivity of rice husk ash in cementitious system, Cons. Build. Materials. 2013; 43:208-216.
24. Darweesh HHM. Characteristics of Portland cement Pastes Blended with Silica Nanoparticles, To Chemistry. 2020; 5:1-14. http://purkh.com/index.php/tochem
25. ASTM-C187-86. Standard Test Method for Normal Consistency of hydraulic Cement, 1993, 148-150.
26. ASTM-C191-92. Standard Test Method for Setting Time of Hydraulic Cement, 1993, 866-868.
27. Neville AM. Properties of Concrete, 5th Edn, Longman Essex (UK), 2011. ISBN: 978-0-273-75580-7 (pbk.). http://www.pearsoned.co.uk.
28. ASTM- C170-90. Standard Test Method for Compressive Strength of Dimension Stone", 1993, 828-830.
29. ASTM-C109M. Standard Test Method for Compressive Strength of Hydraulic Cement Mortars (Using 2-in. Or [50-mm] Cube Specimens), Annual Book of ASTM Standards. ASTM International, West Conshohocken, PA, 2013.
30. Imbabi MS, Carrigan C, McKenna S. Trends and developments in green cement and concrete technology. Int. J. Sustain. Built Environ. 2012; 1:194–216.
31. Darweesh HHM. Geopolymer cements from slag, fly ash and silica fume activated with sodium hydroxide and water glass, Interceram International". 2017; 6(1):226-231. https://doi.org/10.1007/BF03401216
32. Darweesh, HHM. Effect of the combination of some pozzolanic wastes on the properties of Portland cement pastes. iiCL'industria italiana del Cemento. 2005; 808:298-311.
33. Darweesh, HHM. Setting, hardening and strength properties of cement pastes with zeolite alone or in combination with slag, Interceram Intern. (Intern Cer Review), Germany. 2012; 1:52-57.
34. Topçu IB, Ateşin Ö. Effect of high dosage lignosulphonate and naphthalene sulphonate based plasticizer usage on micro concrete properties. Construction and Building Materials. 2016; 120:189–197.
35. Stefanidou M, Papayianni I. Influence of nano-SiO_2 on the Portland cement pastes, Compos. Part B-Eng. 2012; 43:2706–2710.
36. ASTM C618a. Specification for Coal Fly Ash and Raw or Calcined Natural Pozzolan for Use in Concrete. ASTM International, West Conshohocken, USA, 2015.
37. ASTM- C170-90. Standard Test Method for Compressive Strength of Dimension Stone", 1993, 828-830.
38. ASTM-C109M. Standard Test Method for Compressive Strength of Hydraulic Cement Mortars (Using 2-in. Or [50-mm] Cube Specimens), Annual Book of ASTM Standards. ASTM International, West Conshohocken, PA, 2013.
39. Givi AN, Rashid SA, Aziz FNA, Salleh MAM. Experimental investigation of the size effects of SiO_2 nano-particles on the mechanical properties of binary blended concrete, Composites Part B: Engineering. 2010; 41:673-677.
40. Aleem SAE, Heikal M, Morsi WM. Hydration characteristic, thermal expansion and microstructure of cement containing nano-silica, Const. Buil. Mater. 2015; 59:151-160.
41. Darweesh HHM. Mortar Composites Based on Industrial Wastes, International Journal of Materials Lifetime. 2017; 3(1):1-8. http://pubs.sciepub.com/ijml/3/1/1, DOI:10.12691/ijml-3-1-1.

42. Garrett TD, Cardenas HE, Lynam JG. Sugarcane bagasse and rice husk ash pozzolans: Cement strength and corrosion effects when using saltwater. Current Research in Green and Sustainable Chemistry. 2020; 1-2:7-13. https://doi.org/10.1016/j.crgsc.2020.04.003